Competition between exciton-phonon interaction and defects states in the 3.31 eV band in ZnO

D. Tainoff,[1,2,3] B. Masenelli,[1,2,3,*] P. Mélinon,[1,2,3] A. Belsky,[1,2,4] G. Ledoux,[1,2,4] D. Amans,[1,2,4] C. Dujardin,[1,2,4] N. Fedorov,[5,†] and P. Martin[5]

[1]*Université de Lyon, Lyon F-69003, France*

[2]*Université Lyon 1, Villeurbanne F-69622, France*

[3]*LPMCN, CNRS, UMR 5586, Villeurbanne F-69622, France*

[4]*LPCML, CNRS, UMR 5620, Villeurbanne F-69622, France*

[5]*CELIA, Université Bordeaux 1–CNRS–CEA, 351 cours de la Libération, F-33405 Talence Cedex, France*

(Received 23 November 2009; revised manuscript received 22 January 2010; published 4 March 2010)

We investigate the origin of the band at 3.31 eV (A band) commonly observed in the emission spectra of various ZnO samples. This band is of prime importance for the confirmation of *p* doping in ZnO nanostructures. We check the validity of the three main hypotheses generally evoked to explain it in undoped ZnO, namely, surface states, the 1LO phonon replica of the free exciton and a defect-related transition. Using ZnO samples structured at different scales, from macro to nano through meso (i.e., a single crystal, a nanoparticles assembly, and a microcrystalline pellet), we demonstrate that a huge surface/volume ratio does not necessarily imply a strong emission at 3.31 eV, especially for model nanoparticles which are uncapped and synthesized in ultrahigh vacuum. Furthermore, we show that the two other hypotheses are valid and can be at stake concomitantly, according to the quality of the samples. Regarding the 1LO phonon replica of the free exciton, its presence is unambiguously established using a complete model based on an exciton population at thermodynamic equilibrium, including the treatment of the interaction of the excitons with the acoustic phonon bath. We observe that the 1LO phonon replica becomes significant at temperatures higher than 80 K typically. Below this temperature, the 3.31 eV emission is only present in the microcrystalline sample and results from a defect-related transition. Since it is not observed in the nanoparticles that are made from the microcrystals, the possibility of an impurity to be the origin of the invoked defect is unlikely in our experiments. Instead, our study suggests that the defect at stake is of crystalline origin, with an activation energy of 122 ± 5 meV. The related emission is shown to follow a free-to-bound transition mechanism.

DOI: 10.1103/PhysRevB.81.115304 PACS number(s): 78.67.Bf, 78.55.Et, 71.55.Gs

I. INTRODUCTION

In the present decade ZnO has been widely studied in sight of optoelectronic applications. Indeed the high stability of its room-temperature UV excitonic emission, its nontoxicity and its low cost of production make ZnO a good candidate for the realization of UV optoelectronic compounds. However the main barrier to overcome in order to industrialize ZnO optoelectronic compounds is to engineer the doping properties and especially the *p*-doping one. In this context, the possibility for some features of the low-temperature excitonic luminescence to be the optical signature of the *p* doping is a major issue. This is particularly true regarding the controversial assignment to *p* doping of the 3.31 eV band (often called A band) present in the excitonic spectra of various ZnO samples.

Since the energy of the 3.31 eV band is close to the one expected for the optical phonon replica of the free exciton (FX), this band has been first interpreted in this way. On the other hand, the appearance of this band in various kinds of nanostructured samples as dots,[1,2] nanorods,[3] or nanowires[4] has conducted some authors to interpret this feature as a surface contribution. Finally, theoretical studies of some acceptors energies in ZnO have shown that the 3.31 eV band might be related to the presence of acceptor impurities (hence the name "A band" for acceptor band) through different radiative mechanisms like a donor acceptor pair, a free to bound transition or an exciton bound to a defect. Subsequently this band has been seen in a lot of intentionally *p*-doped ZnO samples and it has been tempting to attribute it to the optical signature of *p* doping.[5–8] However the possibility for the acceptor level emission to be due to unintentional impurities or local crystalline symmetry modifications complicates the rigorous assignment of this band to *p* doping. Since the control and the optical signature of the *p* doping is of prime importance, the nature of the 3.31 eV band is of prime importance too.

In order to study the origin of the 3.31 eV band we have made a systematic study of the temperature dependence of the excitonic luminescence of three kinds of ZnO samples which are structured at different scales: from macro to nano through meso scale. The three samples used are a single crystal (macroscale), a microcrystalline powder (mesoscale), and an assembly of ZnO nanoparticles (nanoscale) which are uncapped, controlled in stoichiometry, and crystallinity and deposited in ultrahigh vacuum (UHV). The nanoparticles being made from the microcrystalline powder by a hyperquenching process, we expect to find embedded in them the same impurities as in the microcrystalline powder if they are present in the latter. This enables us to discriminate the influence of impurities from pure size effects, and among the latter the role of the surface states. The emission of these samples is compared to the one of a ZnO single crystal, which is characterized by its long-range crystalline order. Our results show that a huge surface/volume ratio does not necessarily lead to an important emission at 3.31 eV since no such emission is visible in the nanoparticle spectra at 10 K.

Second, the accordance of the temperature dependence of the 3.31 eV band in the single crystal and in the nanoparticle assembly and its fit by a model describing the exciton population at thermodynamic equilibrium, including the influence of the acoustic phonons show that the 1LO phonon replica of the free exciton (1LO-FX) is distinguishable in the 3.31 eV band of ZnO. Eventually, the comparison of the luminescence of the microcrystalline powder at 10 K with the spectra of the two other types of samples, for which the band is absent at the same temperature, reveals that, on top of the 1LO phonon replica, the 3.31 eV band also originates form a defect state (real A band). This feature is ascribed to a free-to-bound (FB) transition.

II. EXPERIMENTS

The three kind of samples studied are a single crystal (SC) from SurfaceNet Gmbh, a microcrystalline (μCs) pellet which has been obtained by sintering (pressing at 15 ton and subsequent annealing at 1000 °C in O_2 atmosphere for 10 h) the 99.999% pure ZnO powder from Cerac and a nanoparticles assembled thin film synthesized by low-energy clusters beam deposition (LECBD).[9] The nanoparticles (NPs) are synthesized by the supersonic quenching of a plasma obtained from the laser ablation of the microcrystal pellet. The nanoparticles are synthesized in the gas phase, with the addition of O_2 in the carrier gas, and then deposited in UHV conditions. The nanoparticles study by transmission electron microscopy (TEM) and x-ray diffraction (XRD) shows that the NPs are crystallized in the wurtzite structure. Using Scherrer's formula, a mean size of 18 nm is deduced from the full width at half maximum of the XRD peaks corresponding to the (100), (002), and (101) plane families. Figure 1 presents the XRD pattern of the film. Two TEM images are also given as an illustration of the individual particles and their assembly that occurs within the film formation, leading to diffracting domains about 18 nm wide as measured with XRD. The stoichiometry of the NPs, controlled *in situ* using x-ray photoelectron and Auger electron spectroscopies, is identical to the μCs one. In both cases no impurity is identified in an amount of 1% or more (the precision of our XPS setup). In addition of the good crystallinity revealed by TEM and XRD, no green luminescence is observed in the NPs cathodoluminescence spectra. This green luminescence is assigned to surface contamination,[10] oxygen vacancies,[11,12] or Cu impurities.[13] More details on the NPs synthesis process, stoichiometry and crystallinity are published elsewhere.[14] The excitonic emission of the samples has been recorded with the experimental setup described in Ref. 15. However, in the present case, we have used the 300 nm (4.13 eV) radiation of a Xe lamp as the excitation source, a 1200 groves/mm grating blazed at 300 nm and a CCD camera of TRIAX 320 spectrometer (Jobin Yvon). The setup resolution we have used was 1 meV. Unless specified, all the spectra shown in this study are normalized to the emission maximum.

III. RESULTS

In the following, we address successively the three main hypotheses evoked to explain the origin of the 3.31 eV band, which are, as mentioned in the introduction, the role of surface states, the 1LO-FX replica and the role of bulk defects, either linked to impurities or to structural faults.

A. Role of the surface

The enhancement of the 3.31 eV emission in various ZnO nanostructures, which are characterized by a large surface/volume ratio, has lead to assign its origin to surface states.[1,16] In this sense, this emission would result from a geometrical-size effect. In order to probe this hypothesis, we compare the excitonic luminescence of a ZnO single crystal and two films of ZnO nanoparticules, one protected by a 200-nm-thick MgO layer (deposited in UHV) and one unprotected. Figure 2 presents the spectra corresponding to two representative temperatures, namely, 10 and 80 K. At 10 K, in all spectra, the excitonic emission is strongly dominated by the donor-bound emission bands called DXs.[17–19] In the 3.33 eV range, the emission exhibits a weak two electron satellite, which involves a DX exciton leaving the donor in an excited state, and some contribution of defects,[17] especially in the case of the MgO-protected nanoparticle film. However, the investigation of this emission is beyond the scope of the present paper. All these peaks have been successfully assigned with respect to the literature.[11,12] In the 3.31 eV region, no emission is detected for any sample. At 80 K, the FX contribution increases to the detriment of the DXs one, corresponding to the thermally activated detrapping of the donor-bound exciton. Concomitantly, the 3.31 eV band appears for the two kinds of samples. The absence of the band in the NPs spectrum at 10 K and its moderate intensity at 80 K seems in contrast with other studies.[11,18] Actually, only a few studies are rigorously concerned with the increase in the 3.31 eV emission yield as the surface/volume ratio increases.[1,2] In most of them, the size of the nanostructures is typically a few tens or hundreds of nanometers, which leads in the best estimate to ratios of about 0.1%. In the case of our nanoparticles, this ratio is more than ten times larger. Therefore, we would expect them to exhibit a significant band at 3.31 eV, which is not the case. Two hypotheses can be evoked to explain this fact: either our peculiar synthesis method (adiabatic supersonic expansion) prevents the formation of the surface defects that may be responsible for the 3.31 eV band or it induces the formations of a majority of nonradiative surface defects with a decay time shorter than the one of the 3.31 eV emission which results in the quenching of this emission. Indeed, it is well known that the outermost layer of a nanostructure (for instance, a shell whose thickness is about the exciton diameter) can be the place of many defects that can have opposite influences. In the present study, it is difficult to tell which hypothesis can prevail. In order to characterize the nanoparticle surface at best, we remind that, whereas the samples of Fallert *et al.* are made by "compressing industrial powders into flat pellets"[1] and those of Fonoberov *et al.*[2] result from wet-chemistry routes, the present NPs are uncapped (no ligand) and their surface has been formed during a drastic cooling process ($\sim 10^{10}$ K/s) and possibly reconstructed in UHV. Their subsequent analysis at air is bound to have induced an adsorption of OH

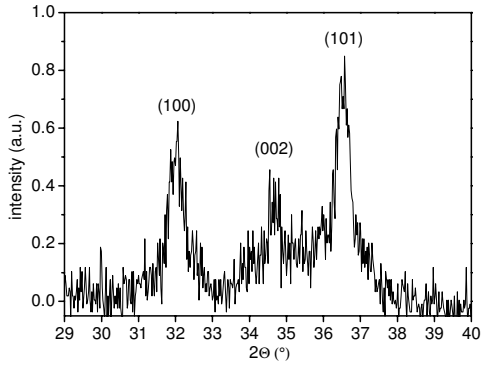

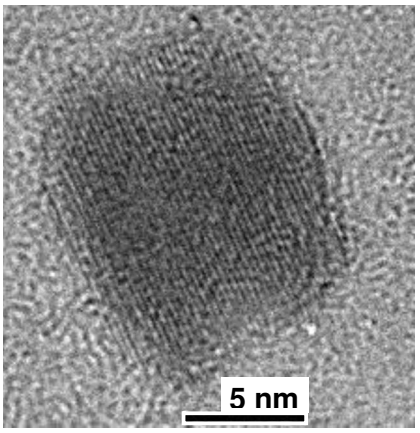

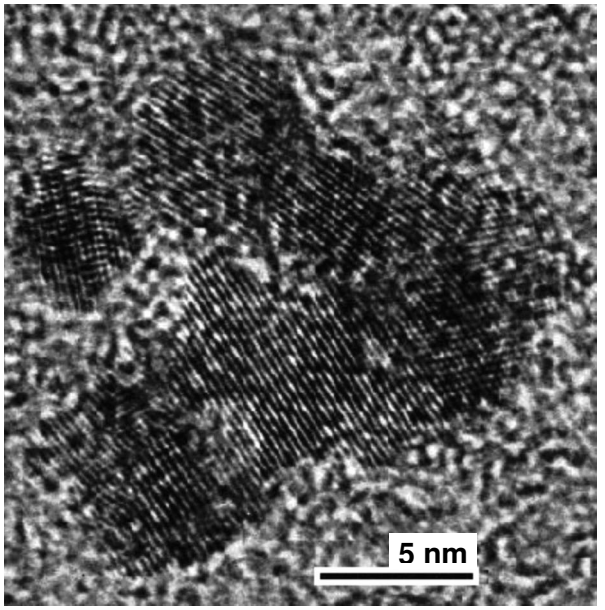

FIG. 1. Upper panel: XRD pattern of the nanoparticle film (excited by the Cu $K\alpha$ radiation). The wurtzite structure is identified by the (100), (002), and (101) peaks. The size of the diffracting domains is deduced from the full width at half maximum of the three peaks using Scherrer's equation. Middle panel: TEM image of an individual particle, the unit building block of the nanostructured sample. Lower panel: example of the assembly of several nanoparticles. Coherent crystalline domains, over 15 nm wide, are clearly distinguished. The scale bar represents 5 nm in the two TEM images.

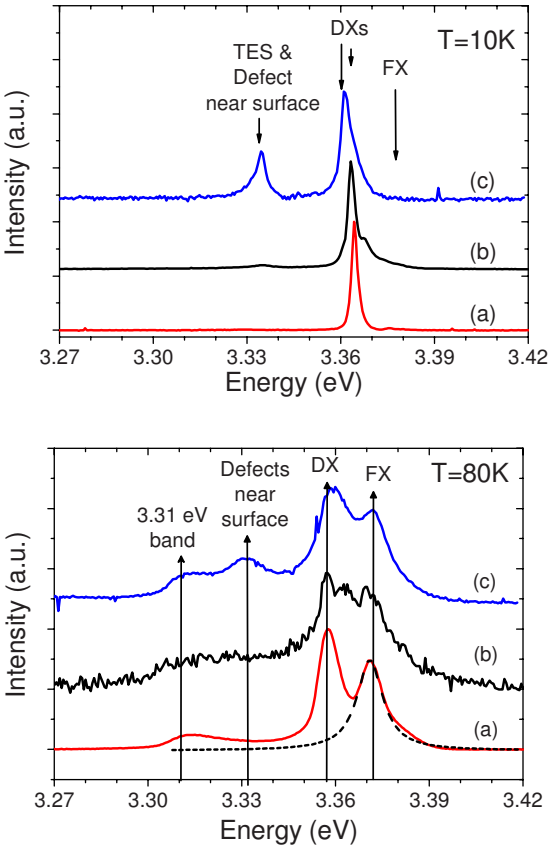

FIG. 2. (Color online) Upper panel: emission spectra at 10 K of (from bottom to top) a ZnO single crystal, an assembly of unprotected nanoparticles, an assembly of nanoparticles protected by a thin MgO film. The excitation wavelength is 300 nm. The absence of the band at 3.31 eV in the nanoparticle sample indicates that its origin is not intrinsically linked to the ZnO surface. Lower panel: emission spectra of the same samples at 80 K. The 3.31 eV band becomes observable.

groups on their surface as is often the case with polar oxide nanoparticles.[20–22] We have checked that the OH contamination does not change the excitonic emission.[23] Besides, as can be seen on Fig. 2, protecting the clusters by an MgO layer does not modify the spectra in the 3.31 eV range. As already mentioned, the only change concerns the defects states responsible for the emission at 3.33 eV. To sum it up, our investigations go to show that increasing the surface/volume ratio does not imply a monotonic increase in the 3.31 eV emission. The discrepancy with other studies seems to be only apparent since the presence, nature and role of surface defects depend on the synthesis method. That is the reason why we only claim that a naked ZnO surface, possibly reconstructed in UHV, does not induce an emission at 3.31 eV.

B. 1LO phonon replica

Highly polar semiconductors, such as ZnO, are known for their significant exciton-phonon coupling.[24] The coupling is strong enough to allow the observation of polaritons even at moderate temperature.[25,26] It is thus sound to contemplate the 1LO phonon replica of the free exciton as the potential origin

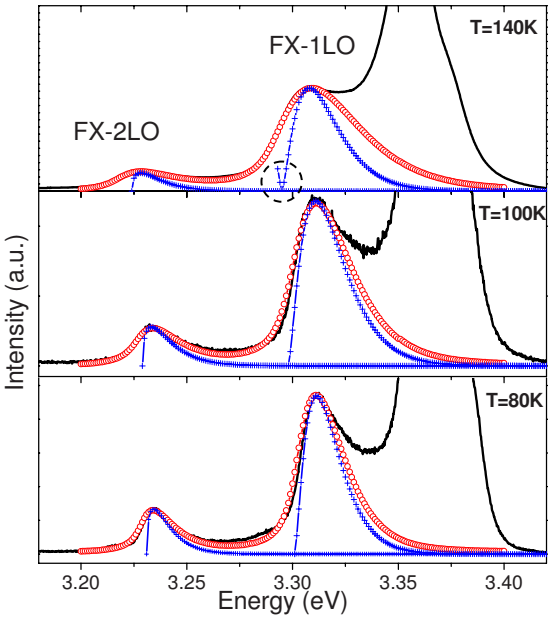

FIG. 3. (Color online) Emission spectra of a ZnO single crystal (solid line) showing the 3.31 eV band and its 1LO replica. The excitation is the 325 nm radiation from a HeCd laser. The two features are modeled as the 1LO and 2LO phonon replicas of the FX contribution by a Permogorov law (cross curve) and a modified Permogorov law taking into account the broadening due to acoustic phonons (circles). The modeling is presented for 80, 100 and 140 K. The cutoff inherent to the Permogorov law is highlighted by a doted circle on the simulation curve for 140 K. Note the improved accuracy in the 3.30 eV region when the Permogorov law is modified by taking into account the interaction of the free exciton with the acoustic phonon bath.

of the 3.31 eV band. The values of the 1LO phonon energy and of the FX energy, being, respectively, 72 meV and 3.37 eV around 80 K, give credit to this hypothesis. One last observation that supports the assignment of the 3.31 eV band to the 1LO-FX replica is the evolution of the band shape with temperature. As shown on Fig. 3 for the single crystal, the 3.31 eV band tends to be more asymmetric on its high-energy side as the temperature increases, which is commonly observed for phonon replicas.[4,27,28] For the particular measurement of the 3.31 eV band evolution with temperature, in order to increase our resolution, we have used a continuous HeCd laser (325 nm) of 0.1 mW for excitation and the spectra have been recorded with an intensified CCD camera coupled to a 3600 groves/mm grating (ARAMIS confocal setup from Jobin Yvon). The resolution of this setup is 0.15 meV and permits us to interpret our line shapes unambiguously. The results obtained from the SC sample are shown in Fig. 3 for three different temperatures. Beside the main DX and FX contributions merged at 3.36 eV, we observe the band around 3.31 eV and another one around 3.23 eV. These two bands can be assigned to the 1LO and 2LO phonon replicas of the free exciton as described hereafter. The most complete model accounting for the exciton-phonon interaction has been given by Segall and Mahan[28] in the formalisms of the Green's functions and even takes into account the polariton bottleneck. However, for an exciton gas in thermodynamic equilibrium, the approach due to Permogorov,[29] which considers a Maxwellian distribution for the kinetic energy of excitons leads to identical results in most of the cases.[30] According to this simplified model, the shapes of the 1LO-FX and 2LO-FX are given, respectively, by the following formulas,[31] where E_{1LO} is the energy of the 1LO phonon and $E_{2LO}=2E_{1LO}$

$$E(\hbar\omega) \propto [\hbar\omega - (E_{FX} - E_{1LO})]^{3/2}\exp\{-[\hbar\omega - (E_{FX} - E_{1LO})]/kT\}, \quad (1)$$

$$E(\hbar\omega) \propto [\hbar\omega - (E_{FX} - E_{2LO})]^{1/2}\exp\{-[\hbar\omega - (E_{FX} - E_{2LO})]/kT\}. \quad (2)$$

The only free parameters are the intensities of the two peaks and the value of E_{1LO}. Figure 3 shows the result of this modeling applied to the SC spectra for different temperatures. The shape of the peak obtained is in qualitative agreement for both the 3.31 eV band and its 1LO replica for temperatures over 80 K. However there is a cutoff in the shape which prevents the modeling of the low-energy part of the peaks. This limitation has been pointed out as soon as the introduction of the exhaustive model by Segall and Mahan.[28] Moreover the result from this modeling is not asymmetric enough to well fit the high-energy tail of both bands. As the discrepancy of asymmetry becomes more pronounced when the temperature increases, we have taken into account the contribution of acoustic phonons, which are a well-known source of broadening. The resolution of our setup being finer than the FX-band full width at half maximum, we can determine the temperature dependence of the acoustic phonons contribution through the homogeneous broadening of the FX transition. In our case FX is fitted with a Lorentzian curve (cf. Fig. 2) and its energy distribution is convolved with the two previous equations in order to obtain a modified Permogorov law taking into account the homogeneous broadening due to acoustic phonons. This procedure has been proposed several times[28,32] but applied only recently.[33] The result of this procedure is presented in Fig. 3. The modified Permogorov model is indisputably better.[34] It is also clear that this approach is quite general and can be used for other semiconductors. This modeling gives us the temperature dependence of the 1LO and 2LO phonon replica energies, which follows the FX temperature dependence. The E_{1LO} energy obtained at different temperatures for the optical phonons is within the 71–73 meV range (cf. Fig. 4) which is in good accordance with both the literature values of 1LO energy determined by Raman spectroscopy[35,36] and our Raman measurements (not presented). This result proves that, if no band is detected at temperatures lower than 80 K, the 3.31 eV band and its 1LO replica that appear at temperatures higher than 80 K are, respectively, the 1LO and 2LO phonon replica of the free exciton. Let us emphasize that all the previous analysis holds also for the NPs sample.

C. Defect-state contribution

Figure 5 presents the emission of the microcrystalline sample at 10 and 80 K (before its use for ablation). Contrary

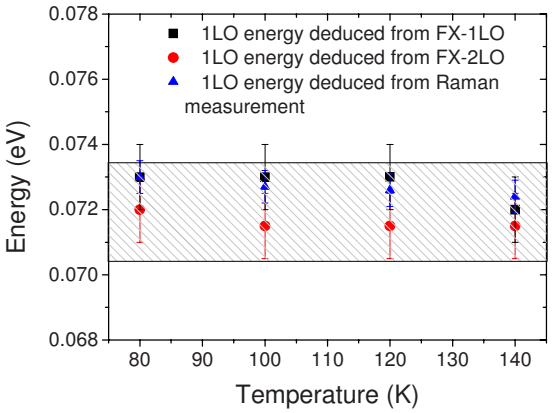

FIG. 4. (Color online) Energies of the longitudinal phonon deduced from the modified Permogorov law applied to emission spectra of the single crystal at different temperatures. The dashed area reproduces the range of suitable phonon energy according to the literature.

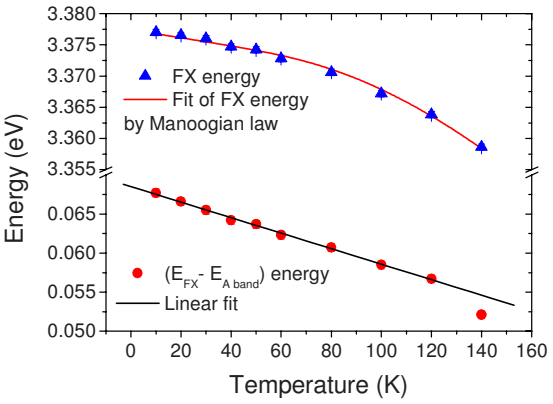

FIG. 6. (Color online) Temperature dependence of the FX energy (triangles) and the corresponding fit using the Manoogian law (solid line). Temperature dependence of the difference in energy between the FX and the A band energies (circles). The variation can be fitted by a linear law, indicative of a free-to-bound transition.

to what is observed for the single crystal and the nanoparticles at 10 K, the peak is observed around 3.31 eV for the microcrystalline sample which cannot be accounted for by the phonon replica of the free exciton. In particular, it does not exhibit the characteristic asymmetric shape. We thus have to consider an electronic defect or an impurity as the possible origin of this band (real A band). This is all the more likely as the band shape can be accurately fit by a Gaussian curve, typical of defect or impurity contributions (see Fig. 5).

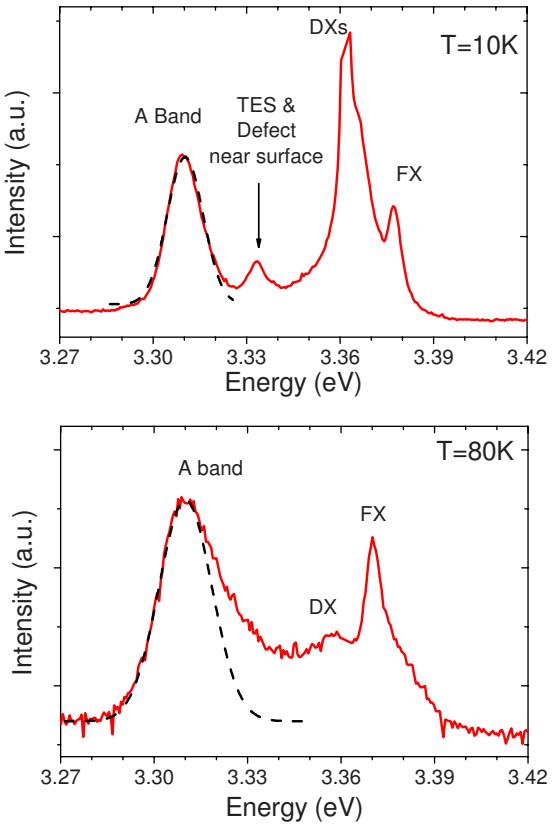

FIG. 5. (Color online) Temperature dependence of the microcrystals excitonic emission. The two dashed lines show examples of fit accuracy for the A band by a Gaussian distribution at 10 and 80 K.

However, the NPs are made from the ablation of the microcrystals of this sample. The ablation results from the interaction of the target with an intense pulsed laser (2×10^6 J per pulse of 10 ns duration, focused on a 1 mm^2 spot, with a 10 Hz repetition rate). The instant energy delivered to the target is so important that the ablation process produces a plasma whose composition is identical to the target one (no selective ablation).[37] Furthermore, the LECBD is a kinetically ruled process, far from the thermodynamic equilibrium. The nucleation of the clusters proceeds via an accretion process with an estimated cooling rate of 10^{10} K/s.[38] At such a drastic cooling rate, the sticking coefficient of the species present in the plasma is close to one,[39] meaning that the clusters assembly has the same stoichiometry as the plasma. Only species that have extremely stable dimers (H_2, O_2, or N_2) are likely to escape from the nucleation process. Even this last statement must be limited when considering weak impurity amounts. Since the accretion is a Poissonnian statistical process, the occurrence of an impurity dimer is very unlikely. Consequently, if an impurity were present in the initial ZnO powder, its luminescent signature would most probably be visible for both the μCs and NPs samples. This is not the case. Therefore, a more likely hypothesis that can be invoked to explain the difference in the spectra of NPs and μCs is a crystalline defect. In order to get more insight into the type of defect, we study the temperature dependence of the 3.31 eV band (A band) in the μCs spectra. The temperature dependence of the position of the defect induced band is generally the method used to differentiate the electronic nature of the defect. The results are exposed in Fig. 6.

The three main mechanisms invoked as possible origins of the defect related band are an exciton bound to an acceptor defect (AX), a donor-acceptor pair recombination (DAP) and a FB transition. For the first two hypotheses the temperature dependence of the transition follows the band-gap-energy variation according, respectively, to[6,31]

$$E_{\mathrm{AX}}(T) = E_g(T) - E_b - E^a_{loc}, \tag{3}$$

$$E_{\mathrm{DAP}}(T) = E_g(T) + E_c - E_a - E_d, \tag{4}$$

where E_{AX} is the energy of the acceptor-bound exciton emission, E_{DAP} the energy of the donor-acceptor pair recombination, E_g the band-gap energy, E_b the binding energy of the exciton, E_a (resp. E_d) the energy of the acceptor (resp. donor) level, E_c the energy of the Coulomb interaction between the donor and the acceptor, and E^a_{loc} the localization energy of the exciton on the acceptor center. Among all these parameters, only E_g depends significantly on the temperature,[31] which implies that the energy dependence of these two transitions follows the FX one. For the temperature dependence of the free-to-bound transition, we have to add a term which models the temperature dependence of the free-electron density of state. Surprisingly, different temperature dependencies have been evoked in the literature for the same mechanism.[4,40,41] The stone mark work of Colbow[40] is well suited for wurtzite-type polar semiconductors and is thus the most justified model in our case. Assuming a parabolic conduction band and a Boltzmann distribution for the free electrons, Colbow writes the temperature dependence of the transition as follows:

$$E_{\mathrm{FB}}(T) = E_g(T) - E_a + \alpha kT \tag{5}$$

with $\alpha = 1$. In our case we have determined the temperature dependence of the band-gap energy by fitting the FX temperature dependence with a Manoogian law[42] as can be seen in Fig. 6. This law is more adapted to the present study than the well-known Varshni law,[43] which is originally demonstrated for cubic materials and is not adapted for fitting the band-gap temperature dependence on a small temperature range. The parameters found here are close to the ones determined by Hamby *et al.*[44] on a ZnO single crystal and their discussion is out of scope of the present study. We then have plotted the temperature dependence of the difference $E_{\mathrm{FX}} - E_{A\ band}$ in Fig. 6. The result, over a 130 K temperature range, clearly shows a linear dependence with $\alpha = 0.97 \pm 0.04$. Since the free-exciton energy follows the gap variation, this confirms the assignment of the band to a free-to-bound transition. Schirra *et al.*[45] have shown that this transition occurs near extended stacking faults in the basal plane. The absence of the 3.31 eV band in the nanoparticles and in the single-crystal spectra at low temperature is in accordance with this hypothesis. Indeed, these stacking faults consist in a change in the crystal symmetry between the wurtzite phase and the zinc blende one, a phenomenon common to hexagonal semiconductors from SiC (Ref. 46) to CdS.[47] They are thus well-defined and extended defects (several nanometers wide). Their presence is unlikely both in an individual cluster of a few nanometers in diameter and in the assembly of such clusters. If not so, it would require some matching of the basal planes between clusters, inducing stacking faults, which we have not observed on a large scale by TEM. Eventually, regarding the single crystal, no large amount of staking faults of the basal plane is to be expected in such a highly crystallized sample. Furthermore, knowing the binding energy of the free exciton ($\sim$60 meV), it is possible to deduce from the temperature dependence of the quantity $E_{\mathrm{FX}} - E_{A\ band}$ the value of the activation energy of the related defect. We obtain the value of 122 ± 5 meV, which is in good accordance with the value of 130 meV reported by Schirra *et al.*[45]

D. Implication for the optical signature of *p* doping

The possibility to use the 3.31 eV emission as an univocal signature of the *p* doping in ZnO structures, and particularly, in nanostructures, is a long-standing issue. As a result of the present study, on top of recent results from the literature,[45,48,49] it appears that this concept is to be used with great caution. Since the 3.31 eV band is partly related to the phonon replica of the FX, the characterization of *p* doping should be first carried out at temperatures below 80 K or so. Second, the absence of any A band (at low temperature) in undoped material should be demonstrated prior to the doping. This would ensure that no defect contributes to the band. Studies from the literature illustrate the fact that the 3.31 eV emission magnitude highly depends on the quality of the sample synthesis. For instance, ZnO nanopillars, with no impurity intentionally incorporated, either grown on sapphire or silicon substrates exhibit an emission at 3.31 eV in the latter case[48] while they do not in the former case.[49] This observation is to be related to the crystalline quality of the samples, which is better in the case of nanopillars grown on sapphire. To further support this, we can mention the absence of the 3.31 eV emission in highly faceted ZnO rods, well crystallized in the wurtzite structure.[50]

It may be argued that, even if the 3.31 eV emission is related to crystalline defects, since these may be of acceptor nature, they naturally contribute to the compensation of the *n*-doping background. Hence, the 3.31 eV band would still be a sound signature of *p* doping. Unfortunately, it seems that the issue is not that simple since scanning capacitance measurements on ZnO layers grown by pulsed laser deposition have shown that regions of *p*-type conductivity coexist with regions of *n*-type conductivity among the same sample.[51] The former regions contain more defects than the latter. This observation tends to limit the role of defects as compensating centers. That is the reason why the ability to synthesize intrinsic samples is a crucial step before achieving *p* doping.

When intentional *p* doping is aimed at, the incorporation of dopants as nitrogen,[7] phosphorus,[5,52,53] or arsenic[54] can be accompanied with the presence of the 3.31 eV emission. Therefore, the link between the incorporation of these elements and the 3.31 eV emission is established. Schirra *et al.*,[45] in their critical review of the literature regarding *p* doping in ZnO, suggest that the previous dopants may induce the formation of crystalline defects (stacking fault of the basal plane) which leads to the appearance of the 3.31 eV emission but not necessarily to a good *p*-type conductivity because of a low-carrier mobility and strong spatial fluctuations of the doping levels.

In this context, our synthesis technique to prepare ZnO nanoparticles is of great interest. They do not exhibit any defect related emission at 3.31 eV. Since their size and their

organization within the sample do not allow for stacking faults of the basal plane which are extended defects, we can exclude that the incorporation of the previously mentioned doping elements would induce such types of defects. Consequently, by incorporating N, P, or As in the nanoparticles, we could probe if the link between the incorporation of *p* dopants and the 3.31 eV emission involves the formation of extended stacking faults. Furthermore, the fact that they are synthesized by a hyperquenching of a hot plasma at a drastic rate [$\sim 10^{10}$ K/s (Refs. 9 and 14)] is a major advantage since it allows us to contemplate the easy incorporation of the usual *p* dopants of ZnO (nitrogen and phosphorus) which is otherwise known to be thermodynamically unstable. Current work is carried out in our group to control this incorporation.

IV. CONCLUSION

We have performed a study of the 3.31 eV excitonic luminescence features using ZnO samples structured at different scales: from macro to nano (i.e., a single crystal, a microcrystalline pellet, and a nanoparticles assembly). At low temperature (10 K), the 3.31 eV band is only present in the microcrystal spectra, in the form a symmetric Gaussian contribution and absent in the single-crystal and nanoparticles spectra. This shows that increasing the surface/volume ratio does not imply a monotonic increase in the 3.31 eV emission yield. It demonstrates that small ZnO nanoparticles free of this emission can be synthesized, even though two distinct reasons for can be argued (absence of radiative surface defects or quenching of these by nonradiative defects). For these two samples, an asymmetric band appears at 80 K and grows bigger as the temperature increases, revealing the presence of the 1LO-FX replica. In order to confirm this statement, we have modeled the line shapes of both the 3.31 eV band and its 1LO replica by a model based on an exciton gas at thermodynamic equilibrium that includes the homogeneous broadening due to acoustic phonons. The modeling, which can easily be extended to other semiconductors, reproduces very accurately the experimental spectra, confirming the assignment of the 3.31 eV band to a phonon replica in these samples. On the other hand, for the microcrystalline sample, the presence of the 3.31 eV band at low temperature points out to an alternate origin, namely, a defect state. Since the nanoparticles are made from the ablation of the pellet via a hyperquenching, the possibility of an impurity to be the origin of the 3.31 eV emission is unlikely in our experiment. Instead, following previous works from the literature, we propose that the corresponding defect could rather be of crystalline origin. The temperature variation in its transition energy suggests a free-to-bound transition emission and gives an activation energy of 122 ± 5 meV. In summary, we emphasize that both the defect hypothesis and the 1LO-FX replica that have been controversially evoked in the literature to explain the origin of the 3.31 eV band in ZnO are concomitantly valid. The growth process, leading to the creation of extended stacking faults is also to be stressed. Eventually, the use of the 3.31 eV band in order to assess *p* doping in ZnO must be invoked with great caution.

ACKNOWLEDGMENTS

This work has benefited from the facilities of the plateforms PLYRA (plateforme lyonnaise de recherche sur les agrégats, http://www-lpmcn.univ-lyon1.fr/plyra/) and CECOMO (center commun de microscopie optique, http://cecomo.univ-lyon1.fr/) of the université de Lyon.

*bruno.masenelli@univ-lyon1.fr

†Present address: Laboratoire des Solides Irradiés LSI/IRAMIS, CEA Saclay, Bt 522, F-91191 Gif Sur Yvette, France.

[1] J. Fallert, R. Hauschild, F. Stelzl, A. Urabn, M. Wissinger, H. Zhou, C. Klingshirn, and H. Kalt, J. Appl. Phys. **101**, 073506 (2007).

[2] V. A. Fonoberov, K. A. Alim, A. A. Balandin, F. Xiu, and J. Liu, Phys. Rev. B **73**, 165317 (2006).

[3] B. P. Zhang, N. T. Binh, Y. Segawa, K. Wakatsuki, and N. Usami, Appl. Phys. Lett. **83**, 1635 (2003).

[4] Q. X. Zhao, M. Willander, R. E. Morjan, Q.-H. Hu, and E. E. B. Campbell, Appl. Phys. Lett. **83**, 165 (2003).

[5] F. X. Xiu, Z. Yang, L. J. Mandalapu, and J. L. Liu, Appl. Phys. Lett. **88**, 152116 (2006).

[6] D. C. Look and B. Claflin, Phys. Status Solidi B **241**, 624 (2004).

[7] D. C. Look, D. C. Reynolds, C. W. Litton, R. L. Jones, D. B. Eason, and G. Catwell, Appl. Phys. Lett. **81**, 1830 (2002).

[8] J. F. Rommeluère, L. Svob, F. Jomard, J. Mimila-Arroyo, A. Lusson, V. Sallet, and Y. Marfaing, Appl. Phys. Lett. **83**, 287 (2003).

[9] A. Perez, P. Melinon, V. Dupuis, B. Prevel, L. Bardotti, J. Tuaillon-Combes, B. Masenelli, M. Treilleux, M. Pellarin, J. Lermé, E. Cottancin, M. Broyer, M. Jamet, M. Negrier, F. Tournus, and M. Gaudry, Mater. Trans. **42**, 1460 (2001).

[10] N. S. Norberg and D. R. Gamelin, J. Phys. Chem. B **109**, 20810 (2005).

[11] A. B. Djurišić and Y. H. Leung, Small **2**, 944 (2006).

[12] Ü. Özgür, Ya. I. Alivov, C. Liu, A. Teke, M. A. Reshchikov, S. Doğan, V. Avrutin, S.-J. Cho, and H. Morkoç, J. Appl. Phys. **98**, 041301 (2005).

[13] N. Y. Garces, L. Wang, L. Bai, N. C. Giles, L. E. Halliburton, and G. Cantwell, Appl. Phys. Lett. **81**, 622 (2002).

[14] D. Tainoff, B. Masenelli, O. Boisron, G. Guiraud, and P. Melinon, J. Phys. Chem. C **112**, 12623 (2008).

[15] G. Ledoux, D. Amans, C. Dujardin, and K. Masenelli-Varlot, Nanotechnology **20**, 445605 (2009).

[16] C. Klingshirn, Phys. Status Solidi B **71**, 547 (1975).

[17] B. K. Meyer, H. Alves, D. M. Hofmann, W. Kriegseis, D. Forster, F. Bertram, J. Christen, A. Hoffmann, M. Straßburg, M. Dworzak, U. Haboeck, and A. V. Rodina, Phys. Status Solidi B **241**, 231 (2004).

[18] A. Teke, Ü. Özgür, S. Doğan, X. Gu, H. Morkoç, B. Nemeth, J. Nause, and H. O. Everitt, Phys. Rev. B **70**, 195207 (2004).

[19] D. C. Look, R. L. Jones, J. R. Sizelove, N. Y. Garces, N. C. Giles, and L. E. Halliburton, Phys. Status Solidi A **195**, 171 (2003).
[20] B. Masenelli, P. Melinon, D. Nicolas, E. Bernstein, B. Prevel, J. Kapsa, O. Boisron, A. Perez, G. Ledoux, B. Mercier, C. Dujardin, M. Pellarin, and M. Broyer, Eur. Phys. J. D **34**, 139 (2005).
[21] H. Zhou, H. Alves, D. M. Hofmann, W. Kriegseis, and B. K. Meyer, Appl. Phys. Lett. **80**, 210 (2002).
[22] C. Wöll, Prog. Surf. Sci. **82**, 55 (2007).
[23] D. Tainoff, B. Masenelli, P. Melinon, A. Belsky, G. Ledoux, D. Amans, C. Dujardin, N. Fedorov, and P. Martin, J. Lumin. **129**, 1798 (2009).
[24] V. V. Ursaki, I. M. Tiginyanu, V. V. Zalamai, V. M. Masalov, E. N. Samarov, G. A. Emelchenko, and F. Briones, J. Appl. Phys. **96**, 1001 (2004).
[25] M. Zamfirescu, A. Kavokin, B. Gil, G. Malpuech, and M. Kaliteevski, Phys. Rev. B **65**, 161205(R) (2002).
[26] R. Kuhnert, R. Helbig, and K. Hümmer, Phys. Status Solidi B **107**, 83 (1981).
[27] M. R. Wagner, P. Zimmer, A. Hoffmann, and C. Thompsen, Phys. Status Solidi (RRL) **1**, 169 (2007).
[28] B. Segall and G. D. Mahan, Phys. Rev. **171**, 935 (1968).
[29] S. Permogorov, in *Excitons*, edited by E. I. Rashba and M. D. Sturge (North-Holland, Amsterdam, 1982), Vol. 177.
[30] S. J. Xu, G. Q. Li, S.-J. Xiong, S. Y. Tong, C. M. Che, W. Liu, and M. F. Li, J. Chem. Phys. **122**, 244712 (2005).
[31] C. Klingshirn, *Semiconductor Optics*, 2nd ed. (Springer, New York, 2005).
[32] T. Makino, Y. Segawa, and M. Kawasaki, J. Appl. Phys. **97**, 106111 (2005).
[33] C. Klingshirn, R. Hauschild, J. Fallert, and H. Kalt, Phys. Rev. B **75**, 115203 (2007).
[34] The only difference between the experiment and the model spectra are localized at the end of the high-energy tail of the phonon replica. These differences are small and likely due to the presence of the phonon replica of the FXB transitions. This transition is visible in the SC spectra at 3.3858 eV (80 K) but it is generally too weak to be taken into account.
[35] R. Cuscó, E. Alarcón-Lladó, L. Artús, J. Ibáñez, J. Jiménez, B. Wang, and M. J. Callahan, Phys. Rev. B **75**, 165202 (2007).
[36] F. Demangeot, V. Paillard, P. M. Chassaing, C. Pagès, M. L. Kahn, and B. Chaudret, Appl. Phys. Lett. **88**, 071921 (2006).
[37] M. Pellarin, E. Cottancin, J. Lerme, J. L. Vialle, J. P. Wolf, M. Broyer, V. Paillard, V. Dupuis, A. Perez, J. P. Perez, J. Tuaillon, and P. Melinon, Chem. Phys. Lett. **224**, 338 (1994).
[38] P. Melinon, V. Paillard, V. Dupuis, A. Perez, P. Jensen, A. Hoareau, M. Broyer, J. L. Vialle, M. Pellarin, B. Baguenard, and J. Lerme, Int. J. Mod. Phys. B **9**, 339 (1995).
[39] A. Benamar, D. Rayane, P. Melinon, B. Tribollet, and M. Broyer, Z. Phys. D: At., Mol. Clusters **19**, 237 (1991).
[40] K. Colbow, Phys. Rev. **141**, 742 (1966).
[41] K. A. Dhese, P. Devine, D. E. Ashenford, J. E. Nicholls, C. G. Scott, D. Sands, and B. Lunn, J. Appl. Phys. **76**, 5423 (1994).
[42] A. Manoogian and J. C. Woolley, Can. J. Phys. **62**, 285 (1984).
[43] Y. P. Varshni, Physica (Amsterdam) **34**, 149 (1967).
[44] D. W. Hamby, D. A. Lucca, M. J. Klopfstein, and G. Cantwell, J. Appl. Phys. **93**, 3214 (2003).
[45] M. Schirra, R. Schneider, A. Reiser, G. M. Prinz, M. Feneberg, J. Biskupek, U. Kaiser, C. E. Krill, K. Thonke, and R. Sauer, Phys. Rev. B **77**, 125215 (2008).
[46] P. Melinon, B. Masenelli, F. Tournus, and A. Perez, Nature Mater. **6**, 479 (2007).
[47] A. Ashrafi and C. Jagadish, J. Appl. Phys. **102**, 071101 (2007).
[48] A. Reiser, A. Ladenburger, G. M. Prinz, M. Schirra, M. Feneberg, A. Langlois, R. Enchelmaier, Y. Li, R. Sauer, and K. Thonke, J. Appl. Phys. **101**, 054319 (2007).
[49] Y. Li, M. Feneberg, A. Reiser, M. Schirra, R. Enchelmaier, A. Ladenburger, A. Langlois, R. Sauer, and K. Thonke, J. Appl. Phys. **99**, 054307 (2006).
[50] W. M. Kwok, A. B. Djurišić, Y. H. Leung, W. K. Chan, D. L. Phillips, H. Y. Chen, C. L. Wu, S. Gwo, and M. H. Xie, Chem. Phys. Lett. **412**, 141 (2005).
[51] H. von Wenckstern, G. Benndorf, S. Heitsch, J. Sann, M. Brandt, H. Schmidt, J. Lenzner, M. Lorenz, A. Y. Kuznetsov, B. K. Meyer, and M. Grundmann, Appl. Phys. A: Mater. Sci. Process. **88**, 125 (2007).
[52] D.-K. Hwang, H.-S. Kim, J.-H. Lim, J.-Y. Oh, J.-H. Yang, S.-J. Park, K.-K. Kim, D. C. Look, and Y. S. Park, Appl. Phys. Lett. **86**, 151917 (2005).
[53] J. D. Ye, S. L. Gu, F. Li, M. Zhu, R. Zhang, Y. Shi, Y. D. Zheng, X. W. Sun, G. Q. Lo, and D. L. Kwong, Appl. Phys. Lett. **90**, 152108 (2007).
[54] Y. R. Ryu, T. S. Lee, and H. W. White, Appl. Phys. Lett. **83**, 87 (2003).